2019-01-1213 Published 02 Apr 2019

Reducing Fuel Consumption by Using Information from Connected and Automated Vehicle Modules to Optimize Propulsion System Control

Pete Olin, Karim Aggoune, Li Tang, Keith Confer, and John Kirwan Delphi Technologies

Shreshta Rajakumar Deshpande, Shobhit Gupta, Punit Tulpule, Marcello Canova, and Giorgio Rizzoni Ohio State University

Citation: Olin, P., Aggoune, K., Tang, L., Confer, K. et al., "Reducing Fuel Consumption by Using Information from Connected and Automated Vehicle Modules to Optimize Propulsion System Control," SAE Technical Paper 2019-01-1213, 2019, doi:10.4271/2019-01-1213.

Abstract

Global regulatory targets and customer demand are driving the automotive industry to improve vehicle fuel efficiency. Methods for achieving increased efficiency include improvements in the internal combustion engine and an accelerating shift toward electrification. A key enabler to maximizing the benefit from these new powertrain technologies is proper systems integration work - including developing optimized controls for the propulsion system as a whole. The next step in the evolution of improving the propulsion management system is to make use of available information not typically associated with the powertrain. Advanced driver assistance systems, vehicle connectivity systems and cloud applications can provide information to the propulsion management system that allows a shift from instantaneous optimization of fuel consumption, to optimization over a route. In the current paper, we present initial work from a project being done as part of the DOE ARPA-E NEXTCAR program. We describe the NEXTCAR program objectives, including the mechanization and build of a demonstration vehicle. As the focus is on real-world fuel economy benefits, the criteria for, and development of, a set of route scenarios is described. In order to be able to develop the necessary optimization logic, and evaluate the benefits on route scenarios beyond those tested in-vehicle, a simulation model of the vehicle and the optimization controls has been developed and is discussed, including correlation testing results and simulated fuel economy benefits. Finally, initial results from the development vehicle running route scenarios on a test track are presented.

Introduction

Global CO2 regulations, in conjunction with customer demand are requiring significant increases in vehicle fuel efficiency. Although all aspects of the vehicle are under scrutiny in this drive to reduce fuel consumption, a particular area of focus continues to be improvements in the powertrain, through both advances in the design of the internal combustion engine, as well as a shift to increasing levels of electrification.

A key enabler for maximizing the benefit from these new powertrain technologies is proper systems integration work - including developing controls that consider the propulsion system as a whole. Thus the focus turns from optimizing the operation of the engine, electrification and transmission controls relatively independently, to considering these as subsystems whose operation is co-optimized by a propulsion system controller.

A next step in the evolution of improving fuel efficiency is a move beyond the powertrain as a closed system, to having the propulsion system controller make use of vehicle level information - information not typically associated with the powertrain operation. The increasing availability of Advanced Driver Assistance Systems (ADAS), Connected and Automated Vehicle (CAV) systems, and access to cloud data makes available to the propulsion controller information that allows it to shift from instantaneous optimization of fuel consumption, to optimization of fuel consumption over a driver's route.

As of 2016 in the USA, 96% of the energy consumed by the transportation sector was generated from fossil fuel sources [1]. This emphasizes the need for cleaner and more efficient forms of transportation. Electrification has been a key enabler for delivering increased efficiency. By 2025, more than 25% of all light duty vehicles are expected to contain some degree of electrification, with most of these being hybrid systems [2, 3]. Several studies have shown the potential of Hybrid Electric Vehicles (HEV's) in reducing fuel consumption [4,5], and that this fuel economy improvement is strongly dependent on the energy management strategy used [6,7,]. A globally-optimal energy management strategy can be realized only with the availability of look-ahead information. ADAS and CAV systems on-board can be utilized to obtain this preview information, to optimize powertrain control as well as the velocity profile followed by the vehicle over a route.

Optimization of the vehicle velocity profile has been explored in the past. For instance, the authors in [8] present an approach to optimize the velocity profile driven by a Battery Electric Vehicle (BEV). A detailed model of the electric machine and battery systems is implemented in a Dynamic Programming (DP) algorithm, which is subject to constraints from road information. Similar work has been done for conventional vehicles (as in [9]). Here, a conventional vehicle is equipped with communication devices which relay current information to a cloud-based algorithm. This computes the optimal velocity that the driver must adopt to be as fuel efficient as possible.

A key element of the optimization problem formulated is often the need for a multi-objective approach, as fuel consumption might not be the only variable or constraint present to consider. For example, [10,11] have implemented minimization functions based on fuel consumed as well as travel time.

In many of the papers presented, for the assurance of a global optimal solution, DP is the optimization method of choice. However, the heavy computation burden of DP has made its use largely limited to asserting an offline performance benchmark. Some research has been conducted, which shows that suitable simplifications to the problem considered can render the DP real-time implementable. This is seen in [12] where an on-board DP controller is implemented, based on direct On-Board Diagnostic (OBD) and GPS signals, to shape the vehicle velocity profile online.

In the current paper, we present work from a project being done as part of the DOE ARPA-E NEXTCAR (Next-Generation Energy Technologies for Connected and Automated On-Road Vehicles) program. We describe the NEXTCAR program objectives, including the mechanization and build of a demonstration vehicle. As the focus is on real-world fuel economy benefits, the criteria for and development of a set of route scenarios is described.

In order to be able to develop the necessary optimization logic, and evaluate the benefits on route scenarios beyond those tested in-vehicle, a simulation model of the vehicle and the optimization controls has been developed and is discussed, including correlation testing results and simulated fuel economy benefits. Finally, initial results from the development vehicle running route scenarios on a test track are presented.

NEXTCAR Program

The goal of the ARPA-E NEXTCAR program [13] is to motivate the development of new and emerging vehicle dynamic and powertrain (VD&PT) control technologies that can reduce the energy consumption of future vehicles through the use of connectivity and vehicle automation. The project target is to achieve at least a 20% reduction in the energy consumption of future connected and automated vehicles (CAVs) compared to a baseline vehicle without these VD&PT control technologies.

Our particular NEXTCAR project involves an integrated concept for the co-optimization of the VD&PT control system that will demonstrate an increase in fuel economy of at least 20% on a light-duty passenger car with a 4-cylinder turbo-charged gasoline direct injection engine, while achieving cost and performance targets. The demonstration vehicle for our project is a 2016 VW Passat with the EA888 engine, up-fitted with a 48V mild hybrid system, an advanced cylinder deactivation technology known as Dynamic Skip Fire (DSF), and CAV technologies.

The partners on the project include The Ohio State University (OSU), which is the project lead, Delphi Technologies, Aptiv, Tula Technology, and the Transportation Research Center (TRC). Together the partners have expertise in propulsion system control, hybrid-electric vehicle (HEV) technology, CAV technology, and vehicle testing.

48V Mild Hybrid System

48V mild hybrid systems are gaining increased acceptance with automotive manufacturers because of the high value the architecture provides in terms of fuel economy and performance improvements, enabling an improved start/stop function, as well as engine torque assist and kinetic energy recovery.

For the project vehicle, the 48V mild hybrid mechanization follows a P0 architecture, as shown in Figure 1, with an engine-mounted Belted Starter Generator (BSG), an inverter, a 48 Volt Lithium Ion battery, and a DC/DC converter.

The 48V stop/start functionality provides a means for fuel economy benefit by shutting the engine off when at prolonged idle such as at a traffic light. When the brake pedal is released, the engine start up is accomplished by the BSG's high torque motor operating through the drive belt of the Front Engine Accessory Drive (FEAD) to turn the engine over. The higher voltage motor provides faster, smoother restart than a 12V system, to achieve reduced NVH and so provide excellent driveability performance.

Stored battery power can also be applied directly to the driving wheels from the BSG via the FEAD and drivetrain to enable engine torque assist.

Energy recovery during vehicle operation is accomplished when a negative torque demand is requested. The Engine Control Module (ECM) commands the inverter to switch the BSG from motoring mode to generating mode so that vehicle kinetic energy is recaptured through the FEAD and converted to stored energy in the battery. The amount of power generated is proportional to the requested negative torque. If the

FIGURE 1 48V Mild Hybrid device layout in NEXTCAR demo vehicle.

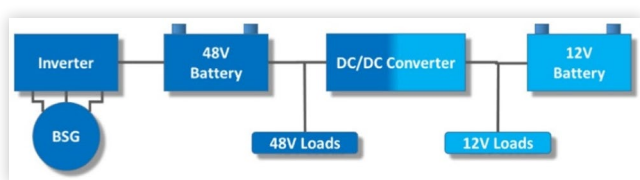

2019 United States Department of Energy.

requested torque is greater than the BSG is capable of absorbing, additional braking is provided by the vehicle's mechanical (friction) brakes.

For the NEXTCAR project, the ability to optimize the recovery and use of vehicle kinetic energy plays a key role in the VD&PT control functions being developed.

Dynamic Skip Fire

Tula Technology's Dynamic Skip Fire (DSF) is an advanced cylinder deactivation strategy providing independent control of each cylinder. With DSF, engine firing decisions are made independently on a cylinder-by-cylinder basis to manage engine torque while firing cylinders at an increased load. This results in a significant reduction in engine pumping losses and improved combustion efficiency compared with standard, throttled engine operation. DSF algorithms determine the number of cylinders to fire to deliver the desired engine torque, and use digital signal processing to manage the frequency of fired and skipped cylinders to maintain excellent noise, vibration and harshness (NVH) characteristics.

An example of DSF operation on a four-cylinder engine is shown in Figure 2. A varying torque request shown in green results in cylinders being fired (red) or skipped (grey). The combined firing density for all four cylinders is shown in blue. When torque demand is near 100%, all cylinders fire. When torque demand is close to zero, 20% or fewer cylinders fire. When torque demand is zero or negative, no cylinders fire; zero cylinders firing is termed Deceleration Cylinder Cut Off (DCCO).

Fuel consumption is reduced substantially, realized primarily through three mechanisms:

1. Elimination of most pumping losses
2. Improved combustion
3. Reduced oxygen saturation of catalysts during deceleration fuel cut events

The DCCO capability of DSF offers additional benefits for hybrid vehicles. While DCCO avoids saturating the catalyst with oxygen during deceleration, it also significantly reduces engine pumping losses (engine braking) during decelerations. By reducing or eliminating engine braking, more of the vehicle's kinetic energy is available for regeneration by the BSG. Therefore, mild hybridization and DSF technologies combine to recuperate more of the vehicle's kinetic energy than has traditionally been available.

FIGURE 2 Dynamic Skip Fire Operation: the green curve shows torque demand [0-100%]; the blue bars give an indication of cylinder firing density; the red and gray cylinders show individual cylinders firing and skipping, respectively.

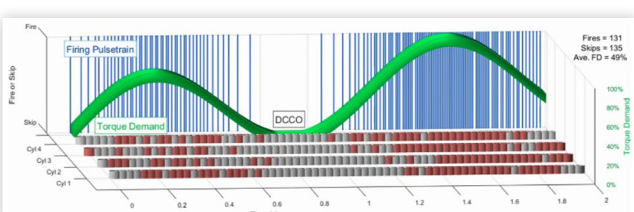

CAV Technologies

CAV technologies on the demonstration vehicle include: an on-board e-horizon module that provides enriched route definition such as road terrain and traffic infrastructure information; a Dedicated Short Range Communication (DSRC) module that enables V2X (vehicle-to-everything) communication including to other vehicles, the infrastructure, and the cloud; and, camera and radar modules to support Adaptive Cruise Control (ACC) capability. In addition, a GPS antenna has been mounted on the vehicle to provide location information.

Project Approach

The focus of our NEXTCAR project is to develop vehicle-level optimization logic and propulsion system controls that use the advanced route information available from the CAV systems on the vehicle in order to determine a vehicle speed profile and a battery energy management profile for the planned vehicle route that together reduce fuel consumption relative to driving that route without incorporating this information. Use of the CAV information allows a fundamental shift in the capability of the propulsion management system, from instantaneous optimization of the control, to optimization of the control over the full route, without sacrificing overall vehicle performance (criteria emissions, drivability, comfort level) or travel time.

The optimized vehicle speed trajectory and battery energy management profiles will also be adapted to optimize the vehicle and propulsion system behavior at traffic lights based on actual traffic signal phase and timing (SPaT), which is obtained from V2I connectivity. By knowing SPaT information, the number of times the vehicle is stopped by a red light can be minimized.

In addition, the route-based, fuel-optimal speed profile will be adjusted to the real-time traffic around the vehicle through the use of information from the radar and camera modules. Finally, stochastic control techniques are being developed and implemented to adapt to the realistic but uncertain surrounding traffic situation with minimal fuel economy degradation.

An experimental automated mechanical braking system has been installed on the vehicle. Combined with the ACC system, it provides the ability to have full longitudinal control of the vehicle, including being able to bring the vehicle to a stop and then accelerate again once the driver indicates it is safe to do so. This gives the project team the ability to evaluate the enhanced vehicle dynamics and powertrain controls, which we refer to as *intelligent driving* (ID) controls, with varying automated driving capability. By automating the vehicle and providing it with the optimal speed trajectory, unnecessary vehicle acceleration and braking can be significantly mitigated compared to a typical driver's velocity profile, with a corresponding improvement in fuel economy.

A rapid prototyping system (RPS) has been integrated into the vehicle as a prototype propulsion control module

FIGURE 3 Representation of the increasing benefits, in terms of reduced energy consumption and so increased vehicle range, as ID controls are integrated with more advanced levels of Automated, Connected and Electrified (ACE) vehicles.

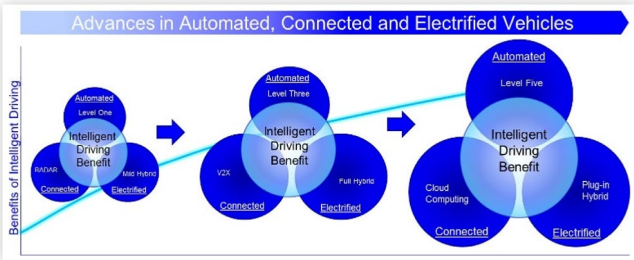

FIGURE 4 Block diagram of 48V P0 Mild-Hybrid Drivetrain

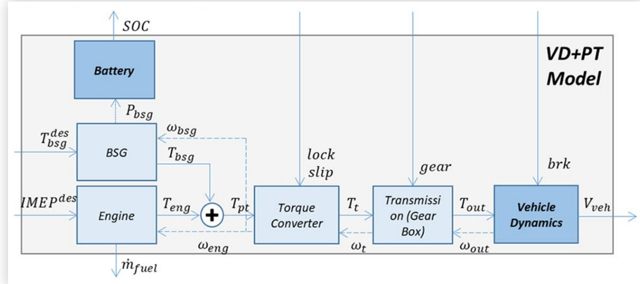

(PCM), in which the functions that optimize the vehicle speed trajectory and battery energy management profile over the route are implemented and tested.

Overall, the concept being developed for the NEXTCAR project combines CAV technology synergistically with a propulsion management system that has a mild hybrid level of electrification, to enable improved fuel economy. With the added CAV systems, the NEXTCAR demonstration vehicle will effectively be at Level 1 automation (based on the SAE J3016 standard), with the control system able to have complete longitudinal control of the vehicle.

With some relatively minor adaptations to the ID controls, however, they are expected to be applicable to vehicles with automated capability from Level 0 to Level 5, and with propulsion systems that include any level of electrification. Figure 3 represents this growing benefit, in terms of advances in Automated, Connected and Electrified (ACE) vehicles. In that sense, the ID controls are layered on top of the level of ACE systems a particular vehicle has.

Model Development and Validation

As a starting point for the project, a model of the vehicle dynamics and powertrain (VD+PT) was developed for fuel economy evaluation over prescribed routes. The model consists of a forward-looking vehicle system simulator that contains a low-frequency dynamic model of the 48V battery pack (for SOC calculation), quasi-static models for the engine (fuel map), BSG (torque and efficiency maps), torque converter and transmission (losses and efficiency calculations), and a low-frequency model of the vehicle longitudinal dynamics (road load equation). This is similar to approaches followed in [14, 15].

The structure of this forward model is shown in Figure 4. To simulate the vehicle and powertrain model, a simplified model of the ECM was developed, based on information and calibration data provided by Delphi Technologies.

The simplified ECM model contains functions which allow conversion from driver inputs to powertrain commands. The inputs from the driver include the accelerator and brake pedal positions. A driver model, which is a velocity reference tracking controller, determines the accelerator and brake pedal positions necessary to follow the desired velocity profile.

The commands to the powertrain from the ECM model are the torque split of desired IMEP ($IMEP^{des}$) and desired BSG torque (T_{bsg}^{des}). $IMEP^{des}$ is an input to the engine model while T_{bsg}^{des} is an input to the BSG model. The torque split is calculated based on a baseline energy management strategy, which also determines the powertrain operating mode (*load shifting, drive assist, or regenerative braking*).

The VD+PT model was then calibrated and verified using experimental data for the FTP drive cycle. The parameters used for calibration include those in the vehicle longitudinal dynamics model, battery model and driver model. These calibration parameters include the vehicle mass, aerodynamic drag coefficient, coefficient of rolling resistance, accessory power load, and proportional and integral gains in the driver model.

Vehicle velocity, gear number, desired BSG torque, battery SOC and fuel consumed are the variables used for validation, by comparing measured values from engine testing to simulation results from the calibrated model. Sample validation results from the engine and simulation over the FTP cycle are shown in Figure 5.

For the vehicle data, the gear number shows as six at the start of the test, because when the vehicle is stationary at the start of the FTP cycle the neutral gear is engaged. The gear number message indicating neutral gear in the CAN data is larger than six; as the upper axis limit in the plot to visualize the gear variable is chosen as six, the neutral gear is shown as gear number six during the start of this cycle. The gear number remains 1 in the model results during this portion as neutral gear has not been modeled and gear number varies from 1-6.

For the FTP cycle, the IMEP matches the experimental data under most conditions. The model also appears to approximate fairly well the gear shifting, BSG torque and battery SOC profiles. The inset plots present a zoomed in view over a select portion of the FTP cycle.

The fuel consumed over the FTP cycle, shown in Figure 6, is well estimated by the model, with error on the final value less than 3.5%, relative to the actual engine. In light of the approximations made and similar models previously developed, the calibration is considered satisfactory for the purpose of predicting fuel consumption and battery SOC profile on user-defined routes.

FIGURE 5 Plots comparing vehicle velocity, gear, engine IMEP, desired BSG torque and battery SOC profiles from the engine and the simulation, run over the FTP cycle, to show model validation; the inset plots present a zoomed in view over a select portion of the FTP cycle.

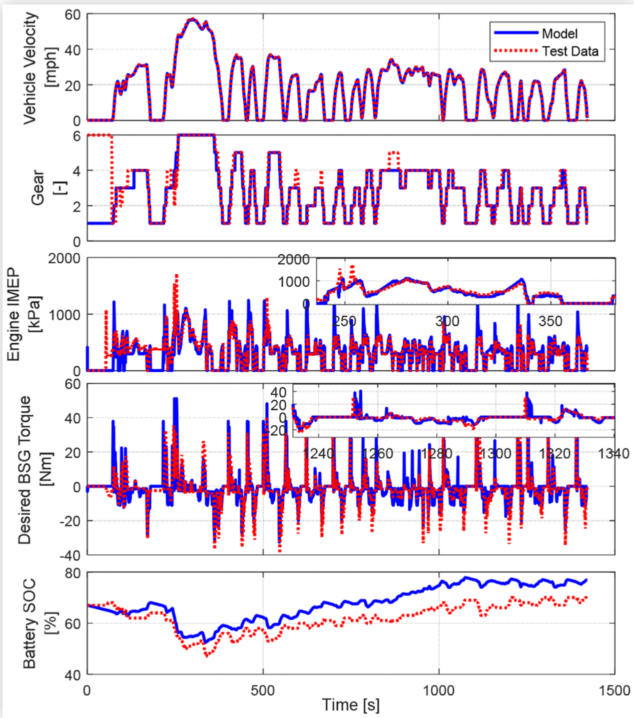

FIGURE 6 Comparison of fuel consumption between model and engine data over FTP cycle; note that the data are shown after cold start is complete to eliminate error due to model not reflecting the production cold start strategy.

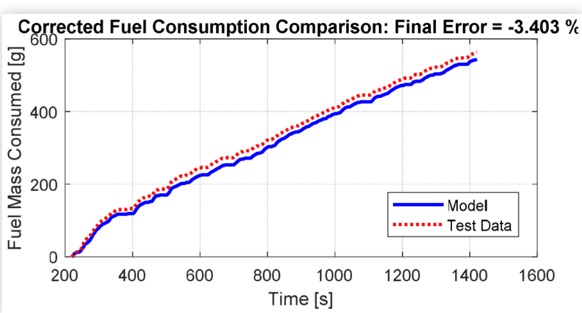

Mismatches in fuel economy are caused by differences in the model of the production powertrain control strategy, which, in particular, does not account for the different calibration of engine and BSG during cold start conditions and leads to an underestimation of fuel consumption in the first 150s of simulation. For that reason, the data in Figure 6 are shown with the errors due to cold start removed, by beginning the comparison at 200s.

Route Scenario Development

To evaluate the performance of the proposed control strategies, information about speed limits, traffic signal locations, and other route characteristics must be provided to the optimization routine. This is done by first defining a route from a starting point to a destination. The route information includes the total trip length, the road grade variation along the route, the maximum and minimum speed limits along the route, and the locations of stop signs and traffic lights.

This information is typically available from enhanced road maps and can be automatically extracted for a given route. It is clear that different route characteristics will have different impacts on fuel consumption and it is therefore important that the set of defined tests represent the various characteristics that might be encountered.

An initial optimization of the vehicle velocity and battery SOC profiles is performed at the beginning of the route, using the information about the route available at that time. For the purpose of this preliminary optimization, all the traffic lights encountered are assumed to be red (i.e., to be stop signs) and no traffic is considered. A more advanced framework for route optimization that considers the impact of varying traffic densities and SPaT has been developed in [19].

To evaluate the optimization algorithms without bias to a particular route or terrain, the selected different driving scenarios should cover a significant variety of operating route and terrain conditions. For characterization of various routes in a statistical manner, some metrics are introduced. The metrics used for evaluation are route speed variance, stop frequency and route grade variance. These metrics are computed for various routes (urban, mixed, and highway) and are plotted on a 3D plot to identify the spread of the route characteristics.

Following [19], *Route speed variance* is formulated as:

$$\sigma_s^2 = \frac{1}{Z}\sum_{i=1}^{Z}\left(S_i - \mu_s\right)^2$$

where Z is the total number of speed limit zones, S_i is the speed limit in each zone and μ_s is the average speed limit. In the route speed variance definition, stop signs and 50% of traffic lights are considered as 0 mph speed limit zones for 10 m (the rest 50% of the lights are considered green and so non-zero speed limit zones). Route speed standard deviation is also calculated as an additional metric.

Stop frequency is defined as:

$$F_s = \frac{1}{N}\sum_{i=2}^{N}\left(x_i - x_{i-1}\right)$$

where, N is the total number of stop signs and traffic lights, and x_i is the position of each stop sign and traffic light. This metric is a measure of how frequently the vehicle must stop in the route.

Route grade variance is defined as:

$$\sigma_g^2 = \frac{1}{D}\int_0^D \left[E(s) - \mu_e\right]^2 ds$$

FIGURE 7 Route map of mixed driving scenario

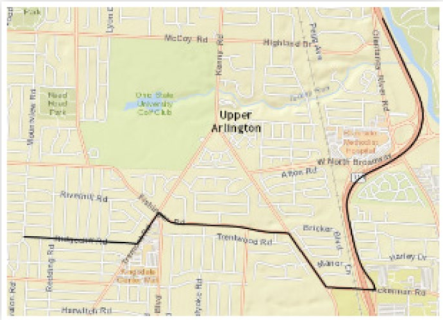

FIGURE 8 Characteristics of mixed (SUMO) Route 19

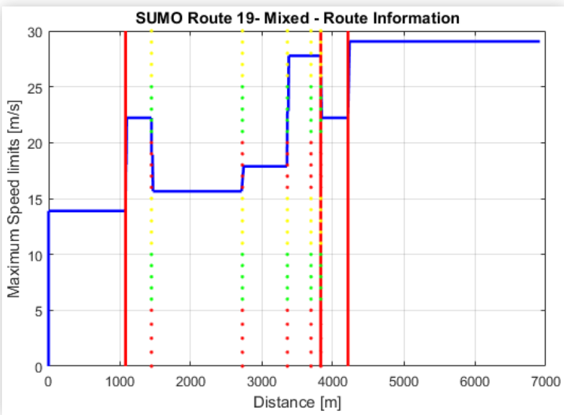

where $E(s)$ is the elevation profile of the route, D is the total route distance and μ_e is the average route elevation,

$$\mu_e = \frac{1}{D}\int_0^D E(s)ds.$$

For the mixed route shown in Figure 7, the speed limits and locations of stop signs and traffic lights are illustrated in Figure 8, in which the blue curve shows the route speed limits, the red lines show the location of the stop signs on the route and the dotted lines show the locations of traffic lights. The total route distance is approximately 6,900 m. This route has an average speed limit of 15.2 m/s (54.8 km/hr), with 5 traffic lights and 3 stop signs. It has a mean road grade of -0.4778 %. Table 1 shows the values calculated for this mixed route.

Some of the urban, highway and mixed routes that have been defined for the metrics calculation are tabulated in Table 2.

The consolidated metrics for the routes shown in Table 2 are listed in Table 3.

TABLE 1 Route characterization metrics for mixed Route 19

Route	Route Speed Variance (m^2/s^2)	Stop Frequency (m)	Route Grade Metric (%)	Average Speed Limit (m/s)	No. of Traffic and Stop Signs
Route 19 (Mixed)	94.43	391.41	0.2099	15.22	5 (T), 3 (S)

TABLE 2 Summary of select routes considered for evaluation of metrics

Route Map	Route Info
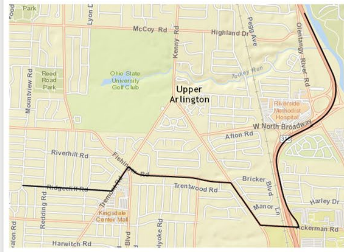	Name: Route 19 **Type: Mixed** Average speed limit: 15.22 m/s; (54.8 km/hr) No. of Traffic signs: 5 No. of Stop signs: 3 Mean grade (in %): -0.4778
	Name: Route 15 **Type: Urban** Average speed limit: 11.66 m/sec; (42.0 km/hr) No. of Traffic signs: 14 No. of Stop signs: 2 Mean grade (in %): 0.2598
	Name: Route 922 **Type: Urban** Average speed limit: 14.30 m/s; (51.5 km/hr) No. of Traffic signs: 11 No. of Stop signs: 2 Mean grade (in %): 0.1989
	Name: Easton Route **Type: Urban** Average speed limit: 13.41 m/s; (48.3 km/hr) No. of Traffic signs: 16 No. of Stop signs: 0 Mean grade (in %): 0.007
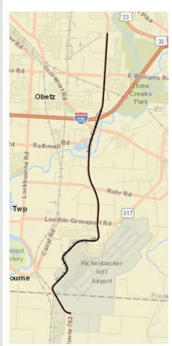	Name: Alum Creek Drive **Type: Mixed** Average speed limit: 16.76 m/s; (60.3 km/hr) No. of Traffic signs: 9 No. of Stop signs: 0 Mean grade (in %): 0.1047
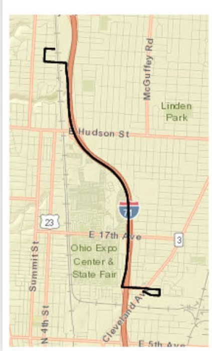	Name: Route 2395 **Type: Highway** Average speed limit: 14.68 m/s; (52.8 km/hr) No. of Traffic signs: 3 No. of Stop signs: 3 Mean grade (in %): -0.1717

TABLE 3 Summary of metrics calculated for select routes considered

Route	Route Speed Variance (m^2/s^2)	Stop Frequency (m)	Route Grade Metric (%)	Average Speed Limit (m/s)	No. of Traffic and Stop Signs
Route 19: Mixed	94.43	391.41	0.2099	15.22	5 (T), 3 (S)
Route 15: Urban	79.77	347.21	0.2090	11.66	14 (T), 2 (S)
Route 922: Urban	102.62	461.02	0.3067	14.30	11 (T), 2 (S)
Easton Route: Urban	136.32	232.25	0.0958	13.41	16 (T), 0 (S)
Alum Creek Drive: Mixed	146.13	743.32	0.0474	16.76	9 (T), 0 (S)
Route 2395: Highway	56.91	691.63	0.4663	14.68	3 (T), 3 (S)

FIGURE 10 Two-parameter analysis of route characterization

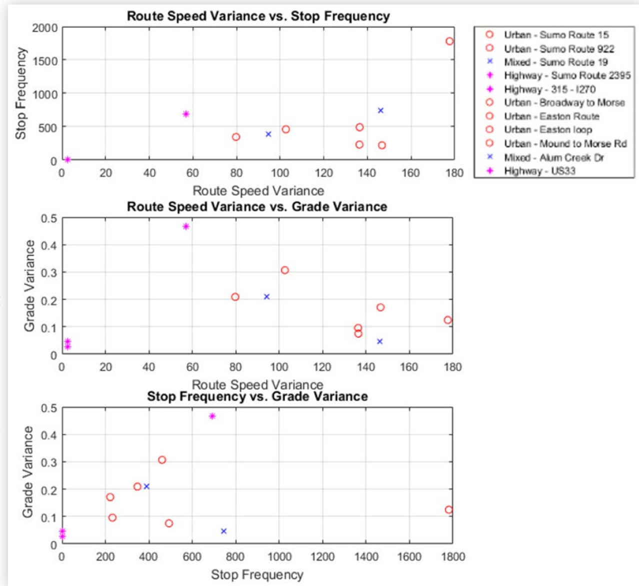

FIGURE 9 Route characterization plot

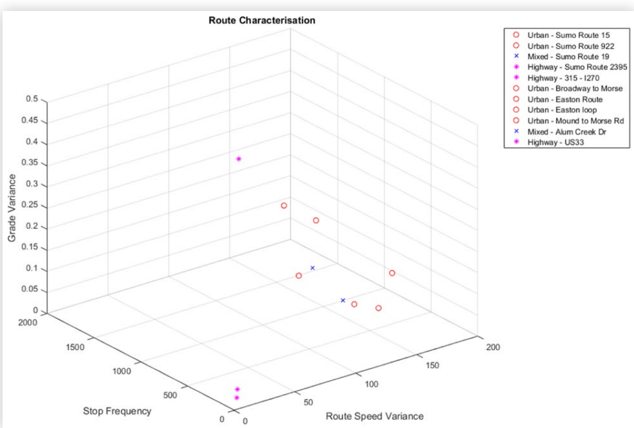

Figure 9 shows a plot of the collection of the metrics calculated for all the routes considered (including those shown in Table 3).

The route characteristics can be further analyzed by studying their behavior considering the parameters pairwise, as is shown in Figure 10. From the Route Speed Variance vs. Stop Frequency subplot in this figure, it is seen that most routes fill up the lower triangle of the graph. This is because the route speed variance and stop frequency are indirectly correlated. Additionally, it can be inferred from the three subplots that considering a few more mixed routes with elevation would better cover the route characteristic space.

Subsequently, any new route can be analyzed using these metrics as described.

Simulation Results

The goal of the VD&PT optimization is to jointly optimize the vehicle velocity profile and powertrain torque split while satisfying route-dependent and state-dependent constraints. Given the complexity of the VD&PT model, which includes nonlinearities due to the efficiency maps of the powertrain components and the presence of the ECU model, Dynamic Programming (DP) was selected as the method of choice to solve the constrained optimization problem.

In order to implement the VD&PT model for numerical solution via DP, the model equations were discretized and expressed in distance-based coordinates, such that the independent variable is distance (instead of time). This is useful for the implementation of stop signs, traffic lights and various other route features in the model, whose positions along the route remain fixed.

The main objective of the optimization is to minimize the fuel consumed over the entire trip. To obtain a non-trivial solution to this problem, the total travel time must be also considered, leading to the following objective function $\boldsymbol{J}$:

$$J(\boldsymbol{x}, \boldsymbol{u}, s) = \min_{\boldsymbol{u}} \sum_{s_i = s_0}^{s_N} \left(\gamma \cdot \dot{m}_f\left(\boldsymbol{x}(s_i), \boldsymbol{u}(s_i), s_i\right) + (1-\gamma) \right) \cdot \frac{\Delta s}{\bar{V}_{veh}(s_i)}$$

where $\boldsymbol{x}$ is the state vector, $\boldsymbol{u}$ is the input vector, $\Delta s (= s_{i+1} - s_i)$ is the distance traveled over one step and $\bar{V}_{veh}(s_i) \left(= \frac{V_{veh}(s_i) + V_{veh}(s_{i+1})}{2} \right)$ is the average velocity over one step. The weight $\gamma \in (0, 1)$ is a tunable penalty factor that can be used to trade-off between the amount of fuel consumed and time taken to complete the route; effectively it constitutes a driving aggressiveness parameter.

The objective function defined above is subject to the following constraints:

$$V_{veh,min}(s_i) \le V_{veh}(s_i) \le V_{veh,max}(s_i)$$
$$SOC_{min} \le SOC(s_i) \le SOC_{max}$$
$$SOC(s_N) = SOC(s_0)$$
$$T_{eng,min} \le T_{eng}(s_i) \le T_{eng,max}$$
$$T_{bsg,min} \le T_{bsg}(s_i) \le T_{bsg,max}$$
$$x(s_{i+1}) = f_{PT}\left(x(s_i), u(s_i), \Delta s, s_i\right)$$

Figure 11 shows the structure of the optimized VD&PT model used for simulation studies. This model integrates the DP results (which are computed offline) with the forward vehicle model. It consists mainly of a *DP Velocity Modifier*, *OSU DP Results* block, the *Simplified ECM* and forward powertrain (or *Plant*) model.

The *DP Velocity Modifier* contains the optimal vehicle velocity profile computed using DP. The *OSU DP Results* block contains the optimal control input trajectories obtained from the optimization routine. The *Conventional Driver* in the block diagram above is a controller to track the desired velocity profile (described previously in the *Model Development and Validation* section). The *Plant* model calculates the fuel as well as other model states.

Evaluation of the optimization strategy developed requires the establishment of a baseline performance. Figure 12 shows the structure of the baseline VD&PT model, comprised mainly of a *Modified Intelligent Driver Model (IDM)*, in addition to the *Simplified ECM* and *Plant* model.

FIGURE 11 Block diagram showing structure of DP-integrated forward model

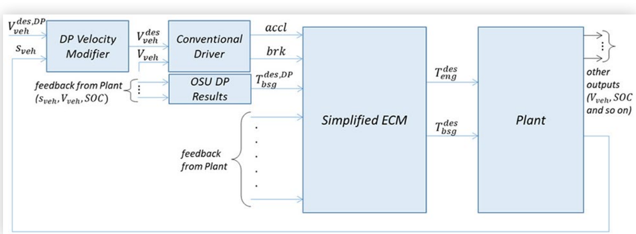

2019 United States Department of Energy.

FIGURE 12 Block diagram showing structure of baseline forward model with modified IDM

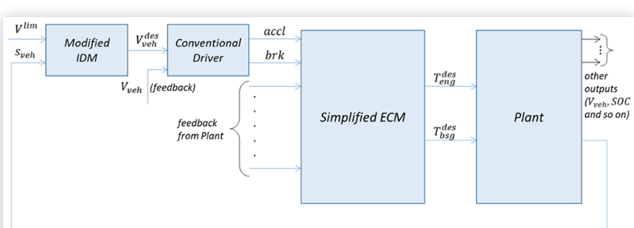

2019 United States Department of Energy.

The *Modified IDM* is based on the Intelligent Driver Model from literature [17, 18], which is a deterministic car-following model for one-lane situations. The *Modified IDM* developed has additional features, enabling its use in the baseline case for CAV testing. Route information such as speed limits and stop signs are fed as inputs to this model. It has been extended to incorporate traffic information such as the presence of a leader vehicle and traffic SPaT.

The *Modified IDM* has been calibrated using real-world data to match the behavior of specific drivers and determine statistically relevant distributions of the model parameters. A sensitivity analysis is then performed on these parameters to obtain a spread of points that represent drivers with different driving styles. This enables determination of the fuel consumption for a real-world driver.

To concisely demonstrate the results from the DP optimization, two routes - Route 19 and Route 15, have been selected from the list shown in Table 2. Figure 13 and Figure 14 show simulation results from Route 19 and 15, respectively, in which the baseline (*IDM DOE*) scatter is compared with the DP-integrated forward model without DSF (*DP Integrated Forward Model*) and the DP-integrated with DSF (*DP-DSF Integrated Forward Model*), for Route 19 and Route 15

FIGURE 13 Comparison of baseline with optimization results for Route 19

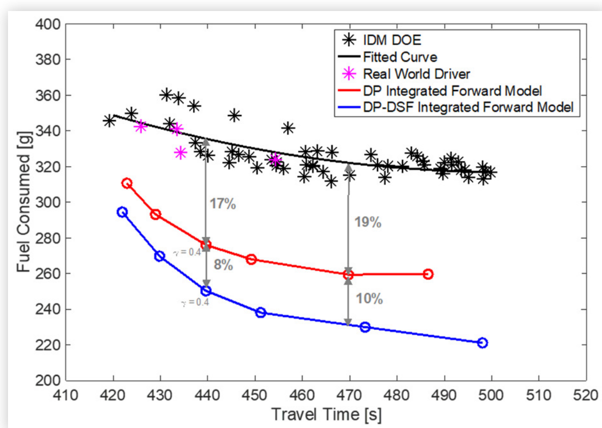

2019 United States Department of Energy.

FIGURE 14 Comparison of baseline with optimization results for Route 15

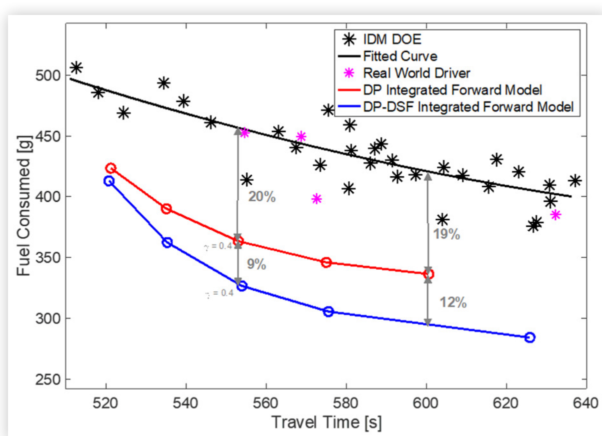

2019 United States Department of Energy.

2019 United States Department of Energy.

respectively. The comparison is performed with respect to the fuel consumed and travel time over a given route.

Here, the baseline model (which includes the *Modified IDM*) is run for different parameters, and the average behavior is considered. *Real-World Driver* behavior is determined using the IDM calibration and has been highlighted in the results (pink markers). The weighting factor, γ in the DP is varied from 0.2 to 0.7 (steps of 0.1) to obtain a Pareto front, as shown below.

Figure 13 shows that that for an average driver, with comparable travel time (of around 440 s), over 17% fuel economy improvement is achieved for Route 19. As Route 15 is an urban route which contains more stops and traffic lights than Route 19, the BSG activity and battery usage is higher. This leads to further improvement (about 20% at around 550s) in the fuel economy over Route 15, as can be seen from Figure 14 . It is to be noted for all these cases shown, SOC neutrality (i.e. charge sustaining operation) is ensured.

Addition of DSF technology to this optimizer further reduces the fuel consumption by over 8% for both Route 19 and Route 15 (at the travel times previously considered). The effects of DSF are captured in simulation mainly through modified fuel consumption and torque converter slip, which are implemented as gear-dependent look-up tables. By suitably shaping the vehicle velocity trajectory and energy management strategy, the DP optimizer synergistically integrates DSF with the rest of the hybrid powertrain. This *pushes* more operating points into the DSF fly-zone than would be possible without the optimization.

NEXTCAR Demonstration Vehicle

A 2016 Volkswagen Passat with a 1.8L TGDi EA888 Gen 3 engine was selected as the base for our NEXTCAR demonstration vehicle build. The base engine was up-fitted with a 48V mild hybrid system, adapted to enable DSF operation, and converted to a Delphi Technologies' powertrain management system. To reflect the current industry trend toward higher injection pressures, the fuel system was converted to a Delphi Technologies production-level 350 bar (Gasoline Direct-injection) GDi fuel system.

ADAS and connected vehicle technologies were integrated into the vehicle, along with a rapid algorithm development system, to support the development of the NEXTCAR optimization functionality. An electronically controlled mechanical braking system was installed to be able to evaluate the ID logic with varying levels of vehicle automation.

The wrapped NEXTCAR development vehicle is shown in Figure 15.

48V Mild Hybrid Mechanization

The demonstration vehicle was up-fitted to a P0 48V mild hybrid configuration, including a Delphi Technologies DC/DC converter. Also included in the P0 architecture are an engine mounted BSG (sometimes referred to as a motor

FIGURE 15 NEXTCAR project vehicle.

generator unit (MGU)) and a 48 Volt Lithium-Ion battery with 8 A-hr working capacity. Figure 1 shows a schematic diagram of the 48V system in the project vehicle.

This P0 configuration adsorbs up to 13 kW during regeneration and delivers up to 10kW as an electric motor. An electric pump was added to maintain transmission pressure during stop/start operation. To increase kinetic energy recovery, vehicle braking was accomplished preferentially through regeneration by the MGU and supplemented, as required, by the production hydraulic friction braking system.

Dynamic Skip Fire

To enable the individual cylinder deactivation required for DSF, an experimental cylinder head was designed and fitted with Delphi Technologies deactivation roller finger followers (dRFF) on the intake and exhaust valves of all cylinders. The dRFF vary valve actuation between full and zero lift to enable cylinder deactivation by switching between a standard cam profile and a base circle cam profile. A hydraulic circuit, controlled by an oil control valve, uses oil pressure to move a pin that engages / disengages a lost motion device in the body of the dRFF.

One deactivation control valve was used for each engine cylinder to control dRFF operation for both intake valves and both exhaust valves for that cylinder. To deactivate a cylinder, a signal is sent to the appropriate oil control valve so that the dRFFs for that cylinder move in lost motion as they ride along the cam profiles; consequently, the valves remain closed. To reactivate the cylinder, the oil control valve releases the oil pressure, a spring forces the pin back into engagement, and the dRFF behaves like a normal type-2 roller finger to open the valve as it rides along the cam profile.

The integration and verification of the combination of DSF with 48V mild hybridization (which when coupled together is called eDSF) was done by Delphi Technologies and Tula Technology. The eDSF concept encompasses the possibility of passive or active torque smoothing, as described in detail in [16]. The NEXTCAR vehicle described here uses a simple implementation of eDSF, with no active torque smoothing. This mechanization enables CO2 reduction benefits, including synergies due to enhanced regeneration and expansion of DSF operation through torque assist. Work continues and further refinement and CO2 reductions are expected.

Propulsion System Controls and Calibration

System control was accomplished using a Delphi Technologies' engine management system (EMS) in a production Delphi Technologies' controller that includes 48V mild hybrid functionality and Tula Technology's DSF algorithms. A Delphi Technologies' transmission control module (TCM) allowed enhanced control of shift schedules and converter slip.

The engine control software in the ECM has been modified to enable the necessary exchange of parameters over CAN with the rapid prototyping system, and also to properly handle the torque split request from the ID controls.

Integration of CAV Technologies

CAV technologies have been installed onto the vehicle by the Aptiv team, and integrated with the propulsion system controls in the rapid prototyping system to support the ID Controls.

A RoadScape eHorizon module is used to provide enriched route information including navigation details, speed limits, locations of stop signs and traffic lights, as well as road slope and curvature. A GPS antenna has been mounted on the vehicle to provide continuous location information.

A Dedicated Short-Range Communication (DSRC) module and antenna have been mounted to the vehicle to enable V2X (vehicle-to-everything) communications. This supports the optimization by the ID logic of the vehicle speed and torque split profiles by providing: enhanced understanding of local traffic conditions around the vehicle through V2V (vehicle-to-vehicle) communication; traffic signal phase and timing (SPaT) status from V2I (vehicle-to-infrastructure) communication to reduce the number of times the vehicle is caught by a red light; and V2C (vehicle-to-cloud) communication. The layout of the additional hardware for the 48V mild hybrid and CAV technologies is shown in Figure 16.

Electronically Controlled Brake

In order to be able to evaluate the ID Controls with different levels of automated driving capability, it is preferable to give the propulsion system controller full longitudinal control of the vehicle. Since the ability to control the brakes through the production electronics was not available to us on our NEXTCAR development vehicle, an experimental electronically-controlled mechanical actuator was installed for this project.

The mechanical actuator consists of a motor that can be commanded to exert pressure on the brake pedal arm. The brake control electronics convert a requested deceleration command into a motor position and so actuate the motor. The

FIGURE 16 Trunk of the NEXTCAR development vehicle, showing some of the 48 Volt Mild Hybrid system and CAV related hardware, and the rapid prototyping system (note that equipment placement in trunk is for development purposes only).

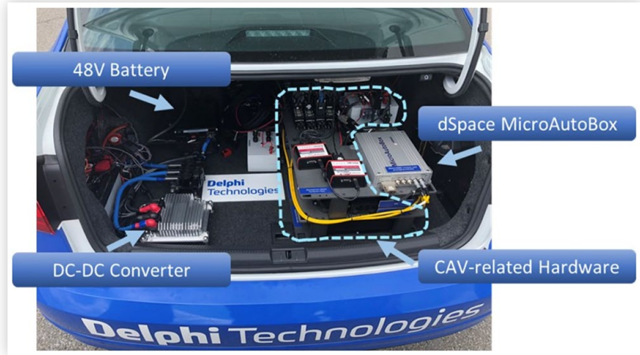

electronically controlled brake is only active when the ID controls are engaged.

Rapid Prototyping System

For implementing and evaluating with the NEXTCAR demo vehicle the potential benefits of the ID controls that are being developed in the simulation work describe above, a Rapid Prototyping System (RPS) was installed by the Aptiv team.

A dedicated computer was integrated into the system to handle the data fusion of the information from the camera and radar modules. A second computer was integrated to drive an in-vehicle monitor showing the acquisition of objects by the ADAS systems. A photograph of the monitor showing the system highlighting traffic signs is shown in Figure 17.

The ID control logic is being executed in a dSPACE MicroAutoBoxII (MABx), along with Aptiv's Adaptive Cruise Control (ACC) logic. The MABx is linked by Ethernet or CAN to the ADAS system computers, as well as the ECM and brake controller.

The ID controls are implemented in SIMULINK. They are compiled using autocode generation, and uploaded to the MABx.

FIGURE 17 Photograph of the in-vehicle monitor showing the ACC system acquiring and highlighting a stop sign and a speed limit sign.

Vehicle Test Results

In this section we discuss the integration of the optimization functions with the existing powertrain controls, the set-up of a route scenario at a test facility for evaluating the potential fuel consumption benefits of the ID controls, and the results obtained from vehicle testing on the defined route.

We include discussion of some of the limitations of the controls and the testing at this point in the project, and point to future directions of the development and testing.

Integration of Optimization Logic

At the heart of the ID controls is the *Optimization Logic*, as shown in Figure 18, which determines the optimal vehicle velocity, as well as the optimal torque split between the IC engine and the electrification system. The optimization is done in a manner that, for the planned route, balances reduced fuel consumption with acceptable travel time. The optimization logic uses current measured and estimated states from the powertrain, as well as information from the CAV modules about the future vehicle route and the current vehicle surroundings.

A *Feature Selection* block distills from the CAV modules the specific information needed for the optimization routines. This information is also used by a *Vehicle Speed Handling* function, which adapts the optimal vehicle speed profile to provide the moment-by-moment desired vehicle speed to the ACC module. The *Final Torque Split* function uses the optimal torque split profile and requested powertrain torque from the ACC module to determine the moment-by-moment torque split command for the ECM.

For the NEXTCAR project, the ID Controls, as well as the ACC logic are contained within the dSPACE MABxII unit.

Test Set-Up

As of the writing of this paper, we are just past the mid-point of the 3-year NEXTCAR project. To-date an initial version of the ID controls have been developed, and the integration of those controls with the ACC module and the ECM has been completed. The version of the logic developed and tested as of the writing of this paper has the following constraints:

- The optimization was completed off-line, and loaded into the dSPACE MABxII; work is on-going to reduce the developed optimization logic to a real-time implementable form, and implement it in the dSPACE.
- The optimization logic only handles speed limit changes and stop signs; work to account for traffic light SPaT in the optimization function is currently in progress.
- The ability to optimize for grade had not yet been included in the optimization at the time of the testing shown.
- The scenario does not include other traffic or obstacles along the route.

In addition, the test track used for evaluation of the ID Controls is not part of our RoadScape eHorizon module, and so the characteristics of the test route were manually integrated into the optimization routine.

The testing was performed at the Kettering University GM Mobility Research Center (MRC) in Flint, Michigan. A lay-out of the MRC facility is shown in Figure 19. The route laid out began and ended at the bottom left corner of the large test pad, looped twice around the oval, for a total distance of 1300 m.

The route shown in Figure 19 was translated into an enriched route characteristics set, based on the measured location of the stop signs (at the middle and end) and the speed limit changes along the route. This route information was then provided to the Optimization routine.

As mentioned above, the Optimization was executed off-line, and the resulting profiles of optimal vehicle velocity and optimal torque split over the route, as a function of current engine state and vehicle location, were loaded into the rapid prototyping system. For the optimization, an aggressiveness parameter γ=0.3 was used. As mentioned previously, this

FIGURE 18 Schematic showing a block diagram of the ID Controls, and there integration with the ACC logic, the ECM and the electronically controlled mechanical braking system.

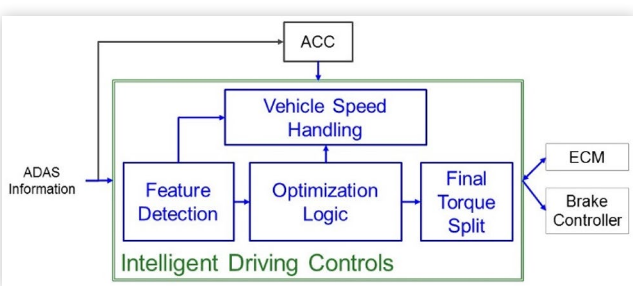

FIGURE 19 Layout of the Kettering University GM Mobility Research Center, where vehicle testing was performed for the results shown in this paper. The blue curve shows the first half of the route, up to the stop sign; the green curve shows the second half of the route, from the stop sign to the end. Placement of the speed limit change signs is not shown, but can be roughly inferred from the x-axis of Figure 20.

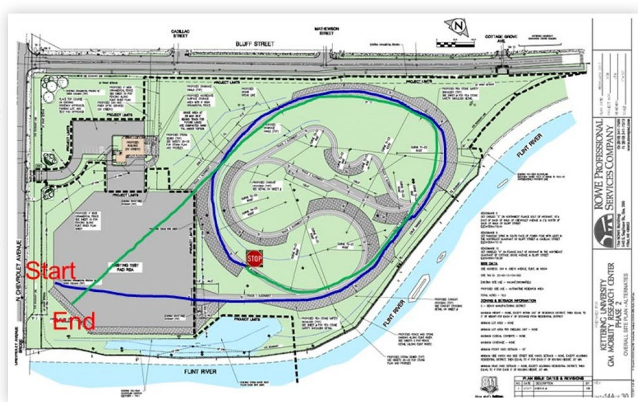

weighting factor produces optimization results that slightly prioritize travel time over fuel consumption, as shown for instance in Figure 13 and Figure 14.

Test Results

A result from the testing is shown in Figure 20, which shows the fuel consumption versus distanced traveled along the route scenario laid out. Along the bottom of the plot, the locations of the speed limit signs and stop sign (roughly mid-route) are shown; note that a stop sign was also located at the end of the route. The figure is from video of the results, in which the fuel consumptions plots were time-synced to a video capture of the car driving the route (upper left) and a video capture of a monitor in the vehicle that displays the ADAS systems capturing information such as traffic signs and other objects along the route.

The plot shows two passes of the NEXTCAR vehicle through the route. The red curve shows the result of the vehicle driving the route with the ID Controls disabled, so the speed is determined by the driver; the blue curve shows the result of the vehicle driving the route with the ID Controls enabled to optimize the vehicle speed and the torque split.

Some observations regarding the results follow. To support the description of the results, snapshots from intermediate points of the video are shown in Figure 21: (a) shortly after the launch of the vehicle; (b) at the stop sign roughly half-way through the course; and (c) at the moment the typical driver has completed the route. As described above, the results are time-sync'd (also with the inset videos); this makes it possible to get a subjective impression of the relative speed with which the vehicles are completing the route in the two cases.

Early in the route, the ID controls have a slower, more conservative vehicle speed than the Typical Driver, while achieving a clear fuel consumption reduction (Figure 21a). More interestingly, the ID Controls cause the vehicle to 'catch-up' with the Typical Driver in the middle of the route, reaching the stop sign at the same time, while continuing to maintain a significant fuel consumption reduction, approximately 15% at the stop sign. Over the second half of the route,

FIGURE 20 Fuel consumption versus distance along route for the scenario tested at MRC. Speed limit signs and stop sign are shown at their location along the course; the route ended at a stop sign. Fuel consumption for a *typical driver* shown in red, and for the *ID controls* shown in blue; the *ID Controls* took 7.8% longer than the *typical driver* took to complete the course, while using 15.1% less fuel.

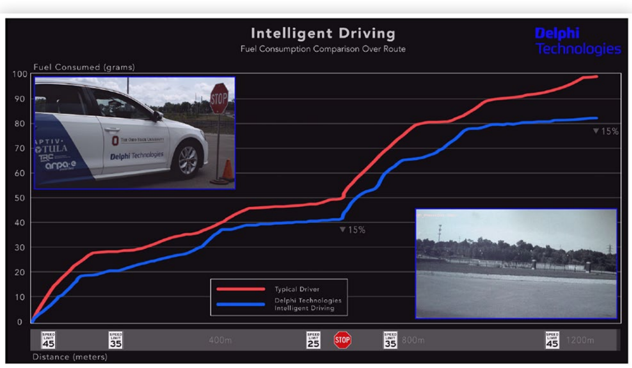

FIGURE 21 Fuel consumption versus distance along route for the scenario tested at MRC, showing intermediate results from the route for the complete data shown in Figure 20: (a) shortly after the launch of the vehicle; (b) at the stop sign roughly half-way through the course; and (c) at the moment the *typical driver* has completed the route. Note that although the ID controls initially lag behind the *typical driver* while achieving a clear reduction in fuel consumption (a), they catch up with the *typical driver* time-wise by the stop sign while maintaining the fuel consumption benefit (b), and finish the course 7.8% later while achieving a final 15.1% fuel consumption benefit, (c) and Figure 20.

(a)

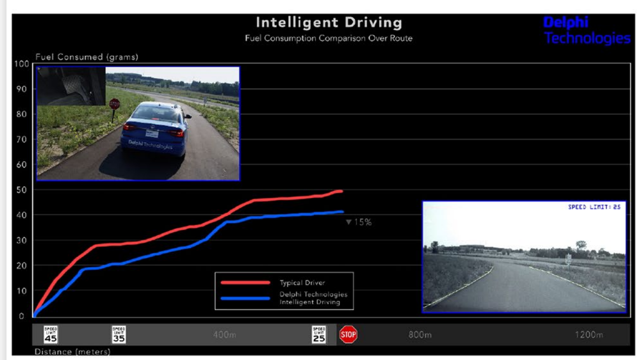

(b)

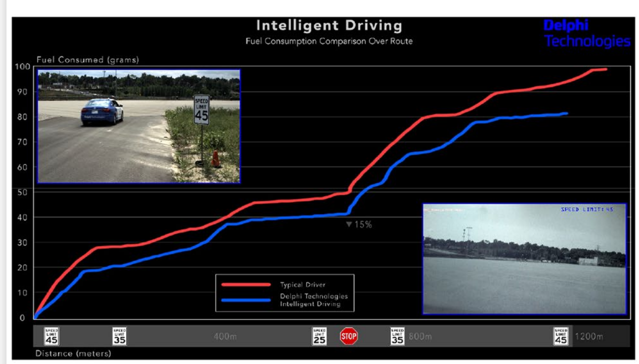

(c)

the ID controls tend to have a slightly more conservative vehicle speed than the Typical Driver, so that the vehicle arrives at the final stop sign with a 7.8% increase in travel time, and the 15% fuel consumption reduction is maintained.

More broadly, it should be understood that the Typical Driver in this stage of the project was driving a constructed course on a relatively short test track, and so had the challenge of trying to 'drive naturally' and simulate how they 'typically' drive on the open road. And, clearly the ID controls will provide a larger reduction in fuel consumption for an aggressive driver versus a conservative driver, as was shown in the section on simulation results.

More testing is underway to establish the range of potential real-world benefits from different drive styles and over a variety of different route scenarios. This work will include: 1) a number of longer route scenarios to be driven at the Transportation Research Center that will represent a variety of typical driving conditions on the open road; 2) a number of different drivers driving the course, and driving it a number of times, to generate a spread for the 'Typical Driver' results; and 3) simulation work to calibrate the simulation driver model based on data from a number of real drivers during their normal driving (i.e., not on specific routes), to then have a correlated driver model for the simulation work.

Summary

Over the next decade, ADAS and CAV technologies with increasing capability are expected to become ever more commonly available on new vehicles. Although these systems are being developed and implemented to improve safety and convenience for customers, the information they make available can be used to improve vehicle fuel economy by providing information about the route to the planned destination.

Knowing the characteristics of the route the vehicle will travel enables a shift from instantaneous optimization of the propulsion system operation to optimization over the route, and so reduced fuel consumption over the route. The benefit of reduced fuel consumption will be most apparent in real-world driving conditions, as standard government test cycles are driven to a defined velocity profile, and do not provide the variation in traffic infrastructure and road topography to allow significant optimization possibilities.

Two megatrends in the automotive industry support this shift to a more optimized propulsion system control through use of the route information. One is the increased electrification of the propulsion system that is expected to occur in response to tightening fuel efficiency regulations. Although a vehicle with only an internal combustion engine can derive benefit from optimized control of the vehicle dynamics based on the route characteristics, adding electrification expands the potential benefit by including in the optimization the capture and use of vehicle kinetic energy in the battery. This potential fuel economy benefit from optimization of the torque split increases, in fact, with increasing battery capacity.

The other applicable megatrend is the increasing level of automation expected in vehicles. Similar to the case of electrification, although fuel consumption benefit can be realized with optimized control of the propulsion system and vehicle dynamics based on the route characteristics on a vehicle with Level 0 automation, the potential benefit increases with increasing levels of automation. As the automation increases --- from ACC systems to full automation --- the propulsion system and vehicle controls are able to more faithfully follow the optimized vehicle speed and torque split profiles, and so realize more of the available benefit.

Our team is investigating these potential benefits in fuel economy through participation in the ARPA-E NEXTCAR program. As part of our project, we have taken a 2016 Volkswagen Passat with a 1.8L TGDi EA888 Gen 3 engine, and up-fitted it with a 48V mild hybrid system, a new cylinder head to enable dynamic skip fire capability, and a Delphi Technologies' engine and transmission management system. We have also added ADAS and CAV modules, and a rapid prototyping system.

The team has developed a calibrated model for the demonstration vehicle propulsion system; variations of this model have been used in both the implementation of the optimization logic for the ID control, as well as in the evaluation of the control in simulation over defined route scenarios. For a specific mixed rural-urban route scenario, we have presented simulation results that show a 15-20% potential reduction in fuel consumption for no increase in travel time when using the ID control.

Testing has also been done in-vehicle, on a route laid out on a test track. The route scenario included speed limit changes and stop signs over a 1300m course. For this route, the ID control was able to achieve a 15.1% reduction in fuel consumption, with a 7.8% increase in travel time, relative to a driver controlling the vehicle speed and with the existing, instantaneous torque split control logic.

These are early results in an on-going project, but they demonstrate the potential benefits available from integrating information from ADAS and CAV modules into the propulsion system controls to optimize operation over a vehicle route. As described in the results section, work continues on incorporating more functionality into the optimization routine. Evaluation of the ID control functions being developed also continues in simulation and in the vehicle.

References

1. U.S. Energy Information Administration, "Monthly Energy Review-January 2018," 2018.
2. IHS Markit, "Light Duty Vehicle Sales Forecast," November, 2018.

3. Goldman Sachs Global Investment Research, “Cars 2025,” 2015.
4. Stockar, S., Marano, V., Canova, M., Rizzoni, G. et al., “Energy-Optimal Control of Plug-In Hybrid Electric Vehicles for Real-World Driving Cycles,” *IEEE Transactions on Vehicular Technology* 60(7):2949-2962, Sept. 2011.
5. Lukic, S.M. and Emadi, A., “Effects of Drivetrain Hybridization on Fuel Economy and Dynamic Performance of Parallel Hybrid Electric Vehicles,” *IEEE Trans. Veh. Technol.* 53:385-389, 2004.
6. Serrao, L., Onori, S., and Rizzoni, G., “A Comparative Analysis of Energy Management Strategies for Hybrid Electric Vehicles,” *ASME. J. Dyn. Sys., Meas., Control.* 133(3):031012-031012-9, 2011.
7. Pisu, P. and Rizzoni, G., “A Comparative Study Of Supervisory Control Strategies for Hybrid Electric Vehicles,” *IEEE Transactions on Control Systems Technology* 15(3):506-518, May 2007.
8. Lu, D., Ouyang, M., Gu, J., and Li, J., “Optimal Velocity Control for a Battery Electric Vehicle Driven by Permanent Magnet Synchronous Motors,” *Mathematical Problems in Engineering* 2014, 2014.
9. Ozatay, E., Onori, S., Wollaeger, J., Ozguner, U. et al., “Cloud-Based Velocity Profile Optimization for Everyday Driving: A Dynamic-Programming-Based Solution,” *IEEE Transactions on Intelligent Transportation Systems* 15(6):2491-2505, 2014.
10. Hellstrom, E., Ivarsson, M., Aslund, J., and Nielsen, L., “Look-Ahead Control for Heavy Trucks to Minimize Trip Time and Fuel Consumption,” *Control Engineering Practice* 17(2):245-254, 2009.
11. Gausemeier, S., Jaker, K. et al., “Multi-Objective Optimization of a Vehicle Velocity Profile by Means of Dynamic Programming,” *IFAC Proceedings Volumes* 43(7):366-371, 2010.
12. Levermore, T., Sahinkaya, M., Zweiri, Y., and Neaves, B., “Realtime Velocity Optimization to Minimize Energy Use in Passenger Vehicles,” *Energies* 10(1):30, 2016.
13. https://arpa-e.energy.gov/?q=arpa-e-programs/nextcar.
14. Eriksson, L. and Nielsen, L., *Modeling and Control of Engines and Drivelines* (John Wiley & Sons, 2014).
15. Sciarretta, A., Back, M., and Guzzella, L., “Optimal Control of Parallel Hybrid Electric Vehicles,” *IEEE Transactions on Control Systems Technology* 12(3):352-363, 2004.
16. Younkins, M., Ortiz-Soto, E., Kirwan, J., Confer, K. et al., “Advances in Dynamic Skip Fire: eDSF and mDSF,” in *27th Aachen Colloquium Automobile and Engine Technology*, 2018.
17. Treiber, M., Hennecke, A., and Helbing, D., “Congested Traffic States in Empirical Observations and Microscopic Simulations,” *Physical Review E* 62(2), 2000.
18. Kesting, A., Treiber, M., and Helbing, D., “Enhanced Intelligent Driver Model to Access the Impact of Driving Strategies on Traffic Capacity,” *Philosophical Transactions of the Royal Society of London A: Mathematical, Physical and Engineering Sciences* 368(1928), 2010.
19. Tamilarasan, S., Jung, D., and Guvenc, L., “Drive Scenario Generation Based on Metrics for Evaluating an Autonomous Vehicle Controller,” SAE Technical Paper 2018-01-0034, 2018, doi:10.4271/2018-01-0034.

Contact Information

Acknowledgments

Our team gratefully acknowledges the support from the United States Department of Energy, Advanced Research Projects Agency - Energy (ARPA-E) NEXTCAR project (award number DE-AR0000794).

Definitions/Abbreviations

ACC - Adaptive Cruise Control
ADAS - Advanced Driver Assistance Systems
ARPA-E - Advanced Research Project Agency—Energy
BEV - Battery Electric Vehicle
BSG - Belted Starter Generator
CAFE - Corporate Average Fuel Economy
CAV - Connected and Automated Vehicles
DCCO - Deceleration Cylinder Cut-Off
DOE - Department of Energy
dRFF - Deactivation Roller Finger Follower
DP - Dynamic Programming
DSF - Dynamic Skip Fire
DSRC - Dedicated Short Range Communication
ECM - Engine Control Module
eDSF - Dynamic Skip Fire with 48V mild hybrid
FEAD - Front Engine Accessory Drive
FTP - Federal Test Procedure
GDi - Gasoline Direct-injection
HEV - Hybrid-Electric Vehicle
ID - Intelligent Driving
IMEP - Indicated Mean Effective Pressure
$IMEP^{des}$ - IMEP desired
MAB - MicroAutoBox (dSPACE)
MGU - Motor Generator Unit
MRC - Mobility Research Center
NVH - Noise, Vibration and Harshness
OBD - On-Board Diagnostic
PCM - Propulsion Control Module
RPS - Rapid Prototyping System
SOC - State of Charge

SPaT - Signal Phase and Timing

T_{bsg}^{des} - Desired BSG Torque

TCM - Transmission Control Module

TRC - Transportation Research Center

V2C - Vehicle-to-Cloud

V2I - Vehicle-to-Infrastructure

V2V - Vehicle-to-Vehicle

V2X - Vehicle-to-Everything

VD&PT - Vehicle Dynamics and Powertrain

ISSN 0148-7191